CHEMISTRY
AN ASIAN JOURNAL
ACES
FULL PAPER

DOI: 10.1002/asia.201402379

Amphiphilic Janus Gold Nanoparticles Prepared by Interface-Directed Self-Assembly: Synthesis and Self-Assembly

Guannan Liu, Jia Tian, Xu Zhang, and Hanying Zhao*[a]

Abstract: Materials with Janus structures are attractive for wide applications in materials science. Although extensive efforts in the synthesis of Janus particles have been reported, the synthesis of sub-10 nm Janus nanoparticles is still challenging. Herein, the synthesis of Janus gold nanoparticles (AuNPs) based on interface-directed self-assembly is reported. Polystyrene (PS) colloidal particles with AuNPs on the surface were prepared by interface-directed self-assembly, and the colloidal particles were used as templates for the synthesis of Janus AuNPs. To prepare colloidal particles, thiol-terminated polystyrene (PS-SH) was dissolved in toluene and citrate-stabilized AuNPs were dispersed in aqueous solution. Upon mixing the two solutions, PS-SH chains were grafted to the surface of AuNPs and amphiphilic AuNPs were formed at the liquid–liquid interface. PS colloidal particles decorated with AuNPs on the surfaces were prepared by adding the emulsion to excess methanol. On the surface, AuNPs were partially embedded in the colloidal particles. The outer regions of the AuNPs were exposed to the solution and were functionalized through the grafting of atom-transfer radical polymerization (ATRP) initiator. Poly[2-(dimethamino)ethyl methacrylate] (PDMAEMA) on AuNPs were prepared by surface-initiated ATRP. After centrifugation and dissolving the colloidal particles in tetrahydrofuran (THF), Janus AuNPs with PS and PDMAEMA on two hemispheres were obtained. In acidic pH, Janus AuNPs are amphiphilic and are able to emulsify oil droplets in water; in basic pH, the Janus AuNPs are hydrophobic. In mixtures of THF/methanol at a volume ratio of 1:5, the Janus AuNPs self-assemble into bilayer structures with collapsed PS in the interiors and solvated PDMAEMA at the exteriors of the structures.

Keywords: gold · interfaces · nanoparticles · polymers · self-assembly

Introduction

Janus particles are a type of nanoparticles with two or more distinct chemical compositions on the surfaces.[1] In the past decade, a number of Janus structures have been synthesized, including Janus silica particles, Janus dendrimers, and Janus micelles.[2] Because of the unique asymmetrical surface structure, the Janus particles present many fascinating properties and have potential applications in self-assembly, surface control, as well as optical and electronic devices.[3,4] For example, Janus particles with opposite electrical charges on two hemispheres could self-assemble into large aggregates,[5] and Janus magnetic nanoparticles with either polystyrene sodium sulfonate or poly[2-(dimethamino)ethyl methacrylate] (PDMAEMA) brushes could form controlled aggregates at low pH values.[6]

Although extensive efforts in the synthesis of Janus particles have been reported, most of the studies focused on particles with sizes in the order of a few tens of nanometers to a few micrometers. The synthesis of sub-10 nm Janus nanoparticles is still challenging. Gold nanoparticles (AuNPs) are the most stable metal nanoparticles and have many unique properties.[7] Janus AuNPs can be used as model Janus structures with sizes in the order of a couple of nanometers. Because of the small size and high electron density, the synthesis and characterization of Janus AuNPs are difficult. For example, a template-assisted method is widely used in the preparation of micron-sized Janus particles; however, it is difficult to find an ideal template for the synthesis of AuNPs in large quantities. In addition, the characterization of Janus AuNPs is also difficult. For example, TEM is one of the most frequently used tools in the characterization of Janus structures. However, because of their high electron density and small size, it is difficult to characterize Janus AuNPs by TEM directly. To date, only a few reports on the synthesis of Janus AuNPs can be found in the literature.[8–13]

Despite the progress achieved in previous research, facile and robust procedures are still desired for the preparation of well-defined Janus AuNPs in large quantities. Herein, a new method for the synthesis of Janus AuNPs is reported. Recently, we established a method to synthesize hybrid colloidal particles or hollow capsules based on interface-directed self-assembly of AuNPs.[14–18] Citrate-stabilized AuNPs

[a] G. Liu, Dr. J. Tian, Dr. X. Zhang, Prof. H. Zhao
Key Laboratory of Functional Polymer Materials
Ministry of Education, College of Chemistry
Nankai University, Collaborative Innovation Center
of Chemical Science and Engineering (Tianjin)
Tianjin 300071 (P.R. China)
Fax: (+86) 022-23498703
E-mail: hyzhao@nankai.edu.cn

Supporting information for this article is available on the WWW under http://dx.doi.org/10.1002/asia.201402379.

were dispersed in aqueous solution and polystyrene (PS) with thiol terminal groups (PS-SH) was dissolved in toluene. A stable emulsion was obtained by mixing the two solutions. Hydrophilic AuNPs interacted with PS-SH through Au–S interactions, and amphiphilic AuNPs were formed at the liquid–liquid interface. PS colloidal particles with AuNPs on the surfaces were prepared by adding the emulsion to excess methanol.[14] A noteworthy feature of the colloidal particles is the decoration of the colloidal particles with AuNPs on the surfaces. The AuNPs were partially embedded in the colloidal particles and the outer regions of the AuNPs were exposed to the medium, so the colloidal particles were perfect templates for the synthesis of Janus AuNPs. The outer regions of the AuNPs on PS colloidal particles were functionalized through the grafting of atom-transfer radical polymerization (ATRP) initiator, 2-bromoisobutyrate ethyl disulfide, through Au–S interactions. After surface-initiated ATRP (SI-ATRP) of 2-(dimethamino)ethyl methacrylate (DMAEMA), Janus AuNPs with PS and PDMAEMA on two hemispheres were prepared. The synthesis of the Janus structures is based on in situ ATRP, so many different polymers can be prepared on AuNPs, and Janus AuNPs with different chemical compositions can be synthesized. Because of the high surface area of the colloidal particles, this template-assisted approach allows the preparation of Janus AuNPs in large quantities. The overall synthetic procedure is shown in Scheme 1.

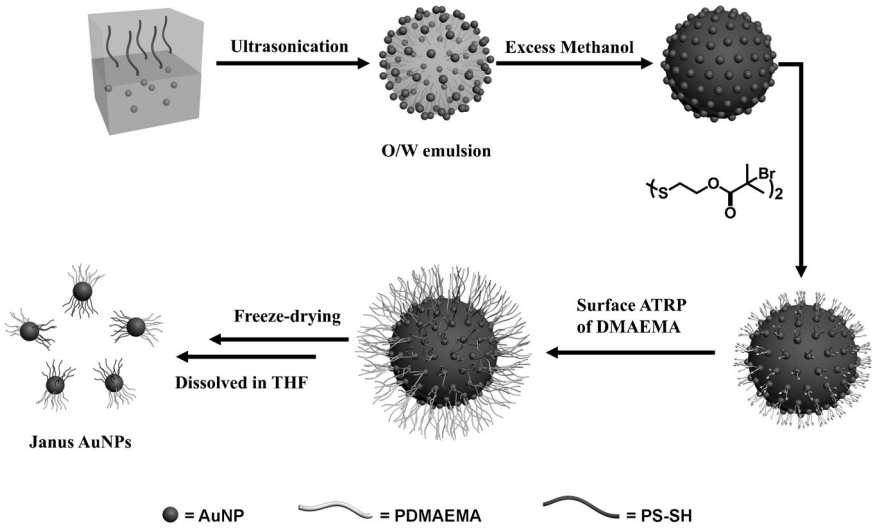

Scheme 1. Outline for the synthesis of Janus AuNPs based on interface-directed self-assembly and SI-ATRP. THF = tetrahydrofuran.

Results and Discussion

Hydrophilic citrate-protected AuNPs prepared in the aqueous phase are able to undergo interface-directed self-assembly in an emulsion with thiol-containing compounds or polymers in the oil phase, and amphiphilic AuNPs are produced at the liquid–liquid interface.[14–17,19,20] Owing to the location of the amphiphilic AuNPs, the stability of the liquid–liquid interface is enhanced and a stable emulsion can be obtained. To realize interface-directed self-assembly of AuNPs, PS-SH was dissolved in toluene, citrate-protected AuNPs were dispersed in the aqueous phase, and the two solutions were mixed together to form an oil/water (o/w) emulsion. After ligand exchange, AuNPs were located at the liquid–liquid interface with anchored PS chains on one side and trisodium citrate on the other side. PS colloidal particles with AuNPs on the surfaces were prepared by adding the emulsion to excess methanol; a solvent that is miscible with both toluene and water.

It is well documented that the aggregation of AuNPs results in a red-shift of the plasmon absorption band owing to electronic coupling interactions between the neighboring nanoparticles.[21,22] Figure 1a shows UV/Vis spectra of citrate-stabilized AuNPs in water, AuNPs aggregated at the

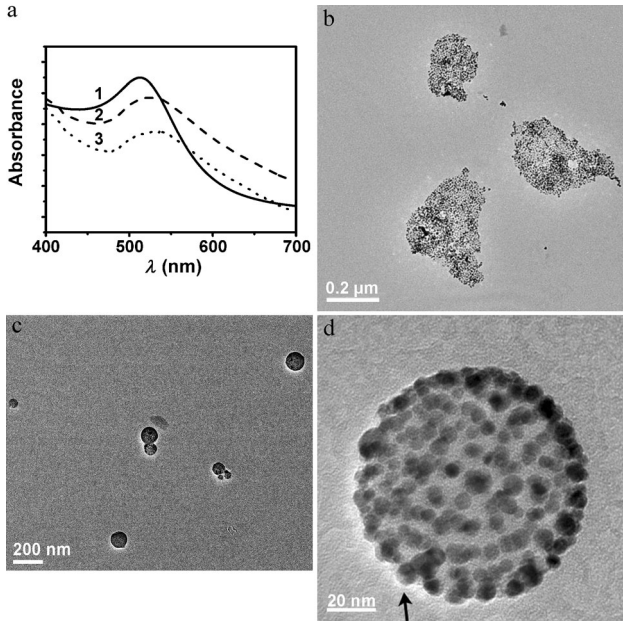

Figure 1. a) UV/Vis spectra of citrate-stabilized AuNPs in water (curve 1), o/w emulsion with PS-SH in toluene and AuNPs in water (curve 2) and PS colloidal particles with AuNPs on the surface (curve 3). b) TEM image of a dried emulsion with citrate-stabilized AuNPs dispersed in the aqueous phase and PS-SH dissolved in toluene. c) and d) TEM images of PS colloidal particles with AuNPs on the surfaces at different magnifications.

liquid–liquid interface, and AuNPs on the surface of PS colloidal particles. The plasmon absorption band of AuNPs in aqueous solution appears with a maximum absorbance at $\lambda = 512$ nm (Figure 1a, curve 1). Owing to aggregation at the liquid–liquid interface, the maximum absorbance of AuNPs in emulsion red-shifts to $\lambda = 524$ nm (Figure 1a, curve 2). The maximum absorbance of AuNPs on the surface of PS colloidal particles appears at $\lambda = 538$ nm, which is 14 nm red-shift in comparison with the AuNPs aggregated at the liquid–liquid interface. The position of the absorption band of the AuNPs is strongly dependent on the size, aggregate state, and refractive index of the medium in which the particles are dispersed.[14,23] The red-shift of the absorption band of AuNPs on the surface of PS colloidal particles is attributed to the change of the environment from the liquid–liquid interface to the solid–liquid surface.[14]

Figure S1 in the Supporting Information shows a TEM image of AuNPs used in this research. The average size of the AuNPs is about 5 nm. Figure 1b shows a TEM image of a dried o/w emulsion with PS-SH dissolved in toluene and citrate-stabilized AuNPs dispersed in aqueous phase. The TEM specimen was prepared by dipping a carbon-coated copper grid into the emulsion and drying in air. In the TEM image, AuNPs aggregate together after evaporation of solvents and no individual AuNPs are observed outside of the droplet structures; this demonstrates self-assembly of AuNPs at the liquid–liquid interface. PS colloidal particles with AuNPs on the surface were prepared by adding the emulsion to a fivefold excess of methanol. Because both toluene and water are miscible with methanol, a homogeneous solution is obtained upon addition of the emulsion to methanol. In solution, PS chains immobilized on the surface of AuNPs through Au–S bonds, collapse forming PS colloidal particles and AuNPs stay on the surface. Figure 1c and d shows TEM images of the colloidal particles at two different magnifications. The TEM results demonstrate that spherical PS particles with AuNPs on the surface are prepared. As indicated by an arrow in Figure 1d, part of an AuNP is embedded in the PS matrix, and the other part is exposed to the solution; this allows further modification.

ATRP initiator, 2-bromoisobutyrate ethyl disulfide, was added to the dispersion of colloidal particles and anchored onto the surface of AuNPs through S–Au bonds. The ^{1}H NMR spectrum of the compound is shown in Figure S2 in the Supporting Information. SI-ATRP of DMAEMA was performed by using CuBr/*N*,*N*,*N*′,*N*″,*N*″-pentamethyldiethylenetriamine (PMDETA) as the catalyst and PDMAEMA polymer chains were synthesized on the surface of AuNPs. To determine the molecular weight of PDMAEMA brushes on AuNPs, sacrificial initiator ethyl 2-bromoisobutyrate was added to the solution. It was reported that free polymers initiated by the sacrificial initiator molecules had almost the same molecular weights as the polymer brushes produced on the solid substrates.[24–27] On the basis of gel permeation chromatography (GPC) results, the apparent number-average molecular weight of PDMEMA is about 23.1 kg mol^{-1}. The colloidal particles, after grafting of ATRP initiator and

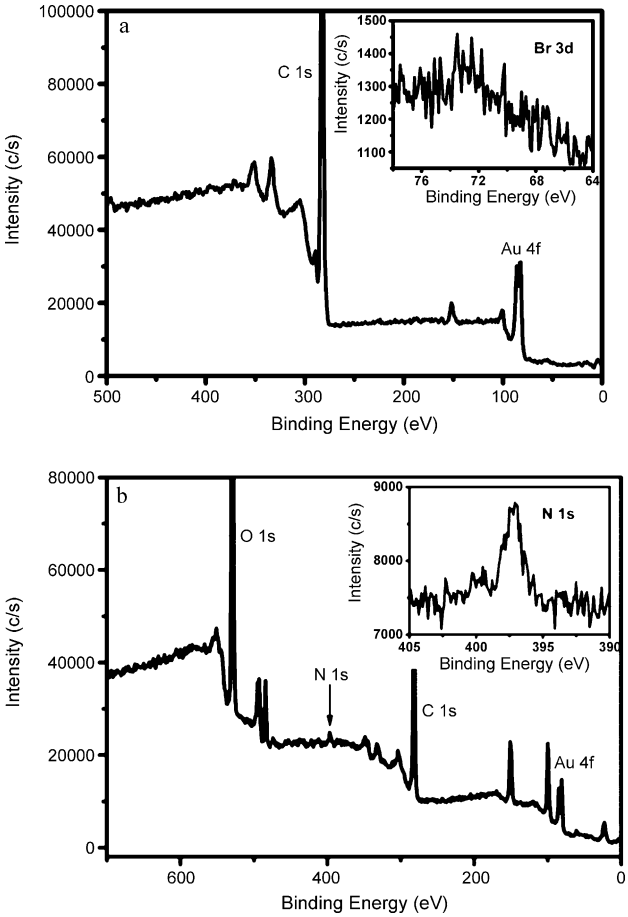

Figure 2. a) Wide XPS spectrum of PS colloidal particles with ATRP initiator anchored on the AuNPs. The inset is the XPS spectrum of Br 3d. b) Wide XPS spectrum of colloidal particles with PDMAEMA on the AuNPs. The inset is the XPS spectrum of N 1s.

SI-ATRP of DMAEMA, were characterized by X-ray photoelectron spectroscopy (XPS). Figure 2a shows the wide XPS spectrum of colloidal particles with ATRP initiator on the AuNPs. In the spectrum, there is a peak at 82.5 eV, which corresponds to the Au 4f binding energy and implies that the surfaces of the colloidal particles are decorated with AuNPs. The Br 3d XPS spectrum is shown in the inset of Figure 2a; the peak at 72.5 eV corresponds to the Br 3d binding energy of the ATRP initiator and demonstrates successful grafting of the ATRP initiator onto the AuNPs. Figure 2b shows a wide XPS spectrum of the colloidal particles after ATRP of DMAEMA on the AuNPs; the inset of Figure 2b gives the N 1s binding energy of PDMAEMA on the AuNPs. In the spectrum, the signal at 397.1 eV corresponds to the N 1s binding energy, which demonstrates the preparation of PDMAEMA brushes on AuNPs by SI-ATRP.

FTIR and ^{1}H NMR spectroscopy results also demonstrate the preparation of PDMAEMA on the surface of AuNPs. Figure S3 in the Supporting Information shows the FTIR spectra of colloidal particles before and after SI-ATRP of DMAEMA. Before SI-ATRP, typical absorption peaks of PS include C–H stretching at $\tilde{\nu} = 3020$ cm^{-1}, aromatic C–C

stretching at $\tilde{\nu}=1460$ and $1600\,cm^{-1}$, C–H out-of-plane bending band at $\tilde{\nu}=760\,cm^{-1}$, and aromatic C–C out-of-plane bending at $\tilde{\nu}=700\,cm^{-1}$ (spectrum a). After SI-ATRP of DMAEMA on AuNPs, the following characteristic bands of PDMAEMA are observed: C–H stretching of the $-N-(CH_3)_2$ groups at $\tilde{\nu}=2830$ and $2770\,cm^{-1}$, C–N stretching of $-N(CH_3)_2$ at $\tilde{\nu}=1150\,cm^{-1}$, and C=O stretching of the ester group of PDMAEMA at $\tilde{\nu}=1729\,cm^{-1}$ (Figure S3 in the Supporting Information, spectrum b).[28] The ^1H NMR spectrum of PS colloidal particles after SI-ATRP of DMAEMA is shown in Figure S4 in the Supporting Information. The chemical shifts at $\delta=4.06$ (signal a) and 2.56 ppm (signal b) are attributed to methylene protons connecting to the ester group and those on the tertiary amine, respectively. The chemical shift at $\delta=2.29$ ppm (signal c) is assigned to the methyl protons connecting to the nitrogen atom on PDMAEMA.

Janus AuNPs with PS and PDMAEMA chains anchored onto two hemispheres were obtained by dissolving the PS colloidal particles in THF followed by centrifugation (Scheme 1). Figure 3a shows a TEM image of the Janus AuNPs. The TEM specimen was prepared by drop-casting a solution of AuNPs/THF on a carbon-coated copper grid. The AuNPs are separated from each other because of the protection of the grafted polymer chains. Direct observation of the asymmetrical surface structure of the Janus AuNPs is difficult owing to the small size of the nanoparticles and high electron contrast between AuNPs and the grafted polymer chains. In previous research, metal NP decoration was used to demonstrate Janus structures.[29,30] For example, we used AuNPs to demonstrate asymmetrical structures of Janus silica particles and Janus Laponite nanosheets.[31,32] PDMAEMA is able to form a complex with metal ions for the in situ synthesis of metal NPs. To demonstrate the asymmetrical structures of Janus AuNPs, we synthesized PtNPs in PDMAEMA domains. Figure 3b and c shows TEM images of Janus AuNPs decorated with PtNPs at two different magnifications. PtNPs with a diameter of about 1.5 to 3 nm are observed on AuNPs; this clearly demonstrates that PS and PDMAEMA cover two different hemispheres on the AuNPs. The surface composition of the PtNP-decorated Janus AuNPs was analyzed by EDX spectroscopy. In the spectrum, the signals corresponding to platinum are detected (Figure 3c). A cartoon showing the structure of a Janus AuNP with PtNPs is presented in the inset of Figure 3c. A control experiment was conducted. In the experiment, ATRP initiator was anchored to the surface of citrate-protected AuNPs and SI-ATRP of DMAEMA was performed on the AuNPs. After ATRP, PtNPs were prepared in PDMAEMA brushes. The TEM results indicated that the PtNPs were distributed around the surface of the AuNPs (Figure S5 in the Supporting Information), which demonstrated that the Janus AuNPs were synthesized in this research.

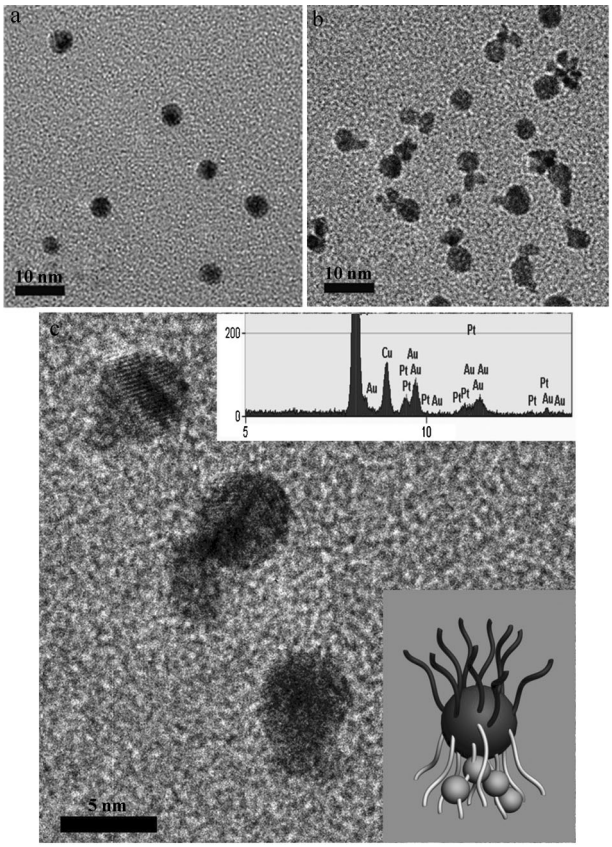

Figure 3. a) TEM image of Janus AuNPs with PS and PDMAEMA on two hemispheres. b) and c) TEM images at different magnifications of Janus AuNPs with PtNPs inside PDMAEMA domains. The insets in c) show the EDX spectrum of PtNP-decorated Janus AuNPs and a cartoon showing the structure of a PtNP-decorated Janus AuNP.

PDMAEMA is a pH-responsive polymer. In acidic pH, the amine groups on the side chains of PDMAEMA are protonated and the polymer is hydrophilic. In basic pH, the side chains of PDMAEMA are deprotonated, which makes the polymer hydrophobic. So, under acidic conditions, Janus AuNPs with PS and PDMAEMA on two opposite sides are amphiphilic and have the behavior of surfactant molecules; under basic conditions, the Janus AuNPs are hydrophobic. Figure 4a shows a photograph of mixtures of toluene/water (1/10, v/v) with Janus AuNPs at two different pH values. At pH 3.0, emulsification of toluene in water by Janus AuNPs is observed. At pH 10.0, the mixture is separated into two immiscible phases, the aqueous and toluene phases, with dispersed AuNPs. The dispersion of the Janus AuNPs in the toluene phase indicates that the Janus AuNPs are hydrophobic and do not have surfactant behavior. Figure 4b shows a TEM image of dried o/w emulsion stabilized by Janus AuNPs at pH 3.0. Spherical aggregations of Janus AuNPs are observed, which demonstrates that the Janus AuNPs are distributed at the liquid–liquid interface at pH 3.0, and the AuNPs aggregate together after evaporation of the solvents. However, when the pH value is increased to 10.0, the hydrophobic Janus AuNPs go into the oil phase and no emulsification can be observed. The surfactant behavior of Janus AuNPs was further demonstrated by optical microscopy. Figure 4c shows an optical microscopy image of a mixture of toluene and water at pH 3.0; toluene droplets in the range

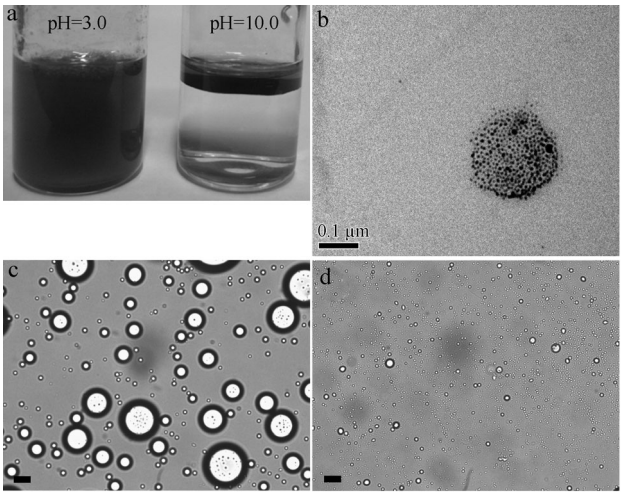

Figure 4. a) Photograph of mixtures of toluene/water (1/10, v/v) with Janus AuNPs at pH 3.0 and 10.0. b) TEM image of dried o/w emulsion prepared at pH 3.0, showing aggregation of Janus AuNPs at the liquid–liquid interface. c) Optical microscopy image of toluene droplets in water (1/30, v/v). d) Optical microscopy image of an emulsion stabilized by Janus AuNPs (0.7 $g L^{-1}$) at pH 3.0. The scale bars in c) and d) represent 50 μm.

from 6.2 to 92.4 μm are observed. However, upon the addition of amphiphilic Janus AuNPs to the mixture, the sizes of the oil droplets range from 3.8 to 17.1 μm (Figure 4d). The reduction in the size of the oil droplets demonstrates that, similar to small-molecule surfactants, the Janus AuNPs are able to reduce interfacial tension between oil and water under acidic conditions.

Janus AuNPs with an asymmetric structure and molecule-like directionality can be used as building blocks in the fabrication of advanced materials. In previous research, van Herrikhuyzen and co-workers prepared Janus AuNPs with hydrophobic alkyl and hydrophilic ethyleneoxide ligands, and they found that Janus AuNPs self-assembled into disk micelles, in which the hydrophobic ligands were in the interior and hydrophilic molecules were at the exterior of the disks.[33] Herein, self-assemblies of Janus AuNPs with PS and PDMAEMA at two hemispheres were investigated in selected solvents. To prepare self-assembled aggregates, Janus AuNPs were dispersed in THF and a fivefold excess of methanol was added to the solution under stirring. Figure 5a shows a TEM image of aggregates self-assembled by Janus AuNPs. The sizes of the assembled structures are in the range of 50–110 nm. A magnified TEM image is shown in Figure S6 in the Supporting Information. Because TEM only provides a two-dimensional projection image of the structures, AFM was used to determine the morphologies of the aggregates. Figure 5b shows a tapping-mode AFM image and a height profile of aggregates self-assembled by Janus AuNPs. A typical aggregate has a diameter of about 82 nm and a thickness of about 9.1 nm. Statistical analysis on the height of the aggregates shows that the average height of the aggregates is about 8.8 nm. It is worth noting that the thickness of the aggregate is about twice that of the average size of AuNPs, which indicates that the Janus AuNPs may self-assemble into bilayer structures. Methanol is a good solvent for PDMAEMA and a precipitant for PS. Upon the addition of excess methanol to a solution of the Janus AuNPs in THF, PS brushes on AuNPs collapse to form the interiors of the structures and solvated PDMAEMA brushes are at the exteriors to stabilize the structures. A cartoon illustrating the bilayer structure of an aggregate is shown in Figure 5c. DLS results also indicated self-assembly of Janus AuNPs in 5:1 methanol/THF. Curve 1 in Figure 5d represents the DLS curve of Janus AuNPs in THF. The average hydrodynamic diameter of the Janus AuNPs is about 21 nm. Curve 2 in Figure 5d represents the DLS curve of the self-assembled structures formed by Janus AuNPs in a 5:1 solution of methanol/THF. The average size of the structures is about 131 nm. Because the solvated PDMAEMA chains collapse during evaporation of the solvents, the sizes of the self-assembled structures measured by TEM and AFM in the dry state are smaller than those obtained by DLS.

The aggregation of AuNPs in the self-assembled structures would result in changes of the optical properties of AuNPs. In comparison to the isolated AuNPs, the plasmon absorption band of the Janus AuNPs in the bilayer structures is red-shifted. Figure 5e shows UV/Vis spectra of AuNPs in aqueous solution, Janus AuNPs in THF, and Janus AuNPs in the bilayer structures. The plasmon absorption bands of AuNPs in aqueous solution and Janus AuNPs in THF are at $\lambda = 512$ (curve 1) and 528 nm (curve 2), respectively. However, upon self-assembly into the bilayer structures, the absorption band of the Janus AuNPs red-shifts to $\lambda = 538$ nm (curve 3). The red-shift of the absorption band is attributed to the aggregation of the Janus AuNPs in the bilayer structures.

Conclusion

PS colloidal particles with AuNPs on the surface were prepared by an interface-directed self-assembly approach. By using the colloidal particles as templates, Janus AuNPs with PS and PDMAEMA on two hemispheres were synthesized by SI-ATRP of DMAEMA. In acidic pH, the Janus AuNPs are amphiphilic and are able to emulsify oil droplets in the aqueous phase. Because of the asymmetric structure, the Janus AuNPs can self-assemble into bilayer structures in selected solvents. This approach could serve as a versatile method for synthesizing Janus AuNPs with tunable optical and electronic properties.

Experimental Section

Materials

DMAEMA (Acros, 99%) was purified by being passed through a basic alumina column, dried over CaH_2, and distilled under reduced pressure. 2,2-Azoisobutyronitrile (AIBN; Guo Yao Chemical Company, 98%) was

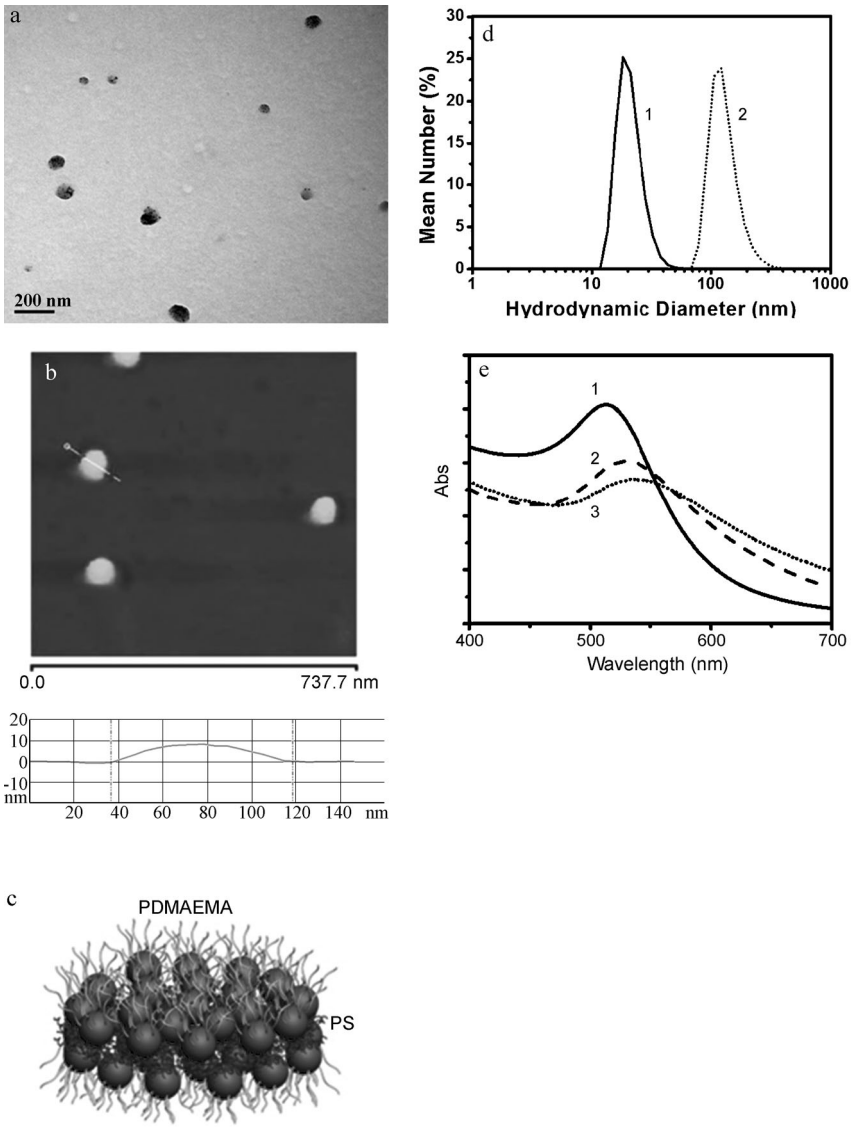

Figure 5. a) TEM image of aggregates self-assembled by Janus AuNPs in a solution of THF/methanol (1/5, v/v). b) A tapping-mode image and a height profile of self-assembled structures of Janus AuNPs in THF/methanol (1/5, v/v). c) A cartoon showing the self-assembled structure of Janus AuNPs. d) Dynamic light scattering (DLS) curves of Janus AuNPs dispersed in THF (curve 1) and self-assemblies of the Janus AuNPs in 5:1 methanol/THF (curve 2). e) UV/Vis spectra of citrate-stabilized AuNPs dispersed in water (curve 1), Janus AuNPs dispersed in THF (curve 2), and self-assembled structures of Janus AuNPs in THF/methanol (1/5, v/v; curve 3).

purified by recrystallization from ethanol. CuBr (99.5%) was purchased from Guo Yao Chemical Company, and purified by being washed with glacial acetic acid and dried in a vacuum oven at 100°C. $HAuCl_4{\cdot}4H_2O$ (Tianjin Chemical Reagent Company, AR), $H_2PtCl_6{\cdot}6H_2O$ (Tianjin Chemical Reagent Company, AR), $NaBH_4$ (Guo Yao Chemical Company, 96%), trisodium citrate dehydrate (Tianjin Chemical Reagent Company, 99%), hydrazine hydrate (Tianjin Rgent Chemicals Co. Ltd., 80%), ethyl 2-bromoisobutyrate (Aldrich, 98%), 2-hydroxyethyl disulfide (Alfa, 90%), 2-bromoisobutyryl bromide (Alfa, 97%), and PMDETA (Aldrich, 99%) were used as received. PS-SH was synthesized as reported previously.[18] The apparent number-average molecular weight and molecular weight distribution of the polymer were 8.6 $kg\,mol^{-1}$ and 1.10, respectively. Details for the synthesis of 2-bromoisobutyrate ethyl disulfide were reported previously.[16] The chemical structure and ^1H NMR spectrum of the compound are shown in Figure S2 in the Supporting Information. The citrate-protected AuNPs were prepared as reported previously.[14] The average size of the nanoparticles was about 5 nm. A TEM image of the AuNPs is shown in Figure S1 in the Supporting Information. All solvents used in this research were distilled before use, and all glassware was immersed in aqua regia before being washed.

Preparation of PS Colloidal Particles with AuNPs on the Surfaces

PS-SH (4.5 mg) dissolved in toluene (1.0 mL) was added to an aqueous dispersion of AuNPs (10 mL, 0.15 $mg\,mL^{-1}$). After sonication, an emulsion was obtained and the solution was stirred at room temperature for 24 h. PS colloidal particles with AuNPs on the surfaces were prepared by adding the emulsion to a fivefold excess of methanol under stirring.

Synthesis of PDMAEMA on the Surfaces of AuNPs

2-Bromoisobutyrate ethyl disulfide (13.6 mg, 0.03 mmol) was added to a dispersion of PS colloidal particles containing AuNPs (1.5 mg). After stirring at room temperature for 48 h, multiple centrifugation processes were applied to remove the free ATRP initiator. The colloidal particles were collected and redispersed in methanol (1.5 mL). DMAEMA monomer (1.0 mL, 5.9 mmol) and sacrificial initiator ethyl 2-bromoisobutyrate (10 μL, 0.06 mmol) were added to the dispersion of the colloidal particles. The mixture was degassed by one freeze–pump–thaw cycle, and a mixture of CuBr (20 mg, 0.13 mmol) and PMDETA (28 μL, 0.13 mmol) in methanol (0.5 mL) was added to the solution under an argon atmosphere. After two freeze–pump–thaw cycles, the polymerization of DMAEMA was performed at 40°C for 24 h. The polymerization was stopped by exposing the solution to air. After centrifugation, colloidal particles were collected and copper ions, ligand, and free PDMAEMA initiated by the sacrificial initiator were removed. Janus AuNPs with PS and PDMAEMA on two hemispheres were obtained by dissolving the colloidal particles in THF followed by centrifugation.

In Situ Synthesis of PtNPs inside PDMAEMA Brushes

$H_2PtCl_6{\cdot}6H_2O$ dissolved in methanol (0.18 mL, 0.02 mM) was added to a dispersion of PS colloidal particles. The dispersion was stirred overnight to allow for equilibration of metal incorporation. Excess ionic species were removed by centrifugation, and metal reduction was performed with hydrazine hydrate (2.4 μL, 80%) under vigorous stirring. Janus AuNPs with PtNPs inside PDMAEMA brushes were obtained by dissolving the colloidal particles in THF followed by centrifugation.

Characterization

The apparent molecular weight and polydispersity of PS-SH were measured on a gel permeation chromatograph equipped with a Hitachi L-2130 HPLC pump; a Hitachi L-2350 column oven operated at 40 °C; three Varian PL columns with 5–600, 500–30, and 100–10 K molecular ranges; and a Hitachi L-2490 refractive index detector. THF was used as the eluent at a flow rate of 1.0 mL min^{-1}. The molecular weight of PS-SH was calibrated on PS standards. TEM observations were performed on a Tecnai G2- F20 electron microscope equipped with an energy-dispersive X-ray spectroscopy (EDS) system and a Model 794 CCD camera. UV/Vis absorption spectra were collected on a Shimadzu UV-2450 spectrophotometer by using a quartz cell of 1 cm path length. XPS spectra were collected on a Kratos Axis Ultra DLD spectrometer with a monochromated $Al_{K\alpha}$ X-ray source ($h\nu = 1486.6$ eV), hybrid optics, a multichannel plate, and delay line detector. An aperture slot with a size of 300 × 700 μm was used in the measurements. Survey spectra and high-resolution spectra were recorded with pass energies of 160 and 40 eV, respectively. FTIR spectra were collected on a Bio-Rad FTS 6000 system by using diffuse reflectance sampling accessories. DLS measurements were conducted on a Malvern Zetasizer Nano-ZS instrument equipped with a 10 mW HeNe laser at a wavelength of 633 nm. The results were analyzed in CONTIN mode. AFM images were collected on a Nanoscope IV atomic force microscope (Digital Instruments Inc.). The microscope was operated in tapping mode by using a silicon tip on a nitride lever with a resonance frequency of 50–80 kHz. The voltage was between 2 and 3 V, and the tip radius was 2–12 nm. A drive amplitude of 1.2 V and a scan rate of 1.0 Hz were used.

Acknowledgements

This project was supported by the National Natural Science Foundation of China (NSFC) under contract 21174073, the National Basic Research Program of China (973 program, 2012CB821500), and PCSIRT (IRT1257).

[1] a) J. Hu, S. Zhou, Y. Sun, X. Fang, L. Wu, *Chem. Soc. Rev.* **2012**, *41*, 4356–4378; b) K. J. Lee, J. Yoon, J. Lahann, *Curr. Opin. Colloid Interface Sci.* **2011**, *16*, 195–202; c) G. Loget, A. Kuhn, *J. Mater. Chem.* **2012**, *22*, 15457–15474.

[2] a) S. Berger, A. Synytska, L. Ionov, K. J. Eichhorn, M. Stamm, *Macromolecules* **2008**, *41*, 9669–9676; b) J. Zhang, X. Wang, D. Wu, L. Liu, H. Zhao, *Chem. Mater.* **2009**, *21*, 4012–4018; c) D. Suzuki, S. Tsuji, H. Kawaguchi, *J. Am. Chem. Soc.* **2007**, *129*, 8088–8089; d) F. Wurm, A. F. M. Kilbinger, *Angew. Chem.* **2009**, *121*, 8564–8574; *Angew. Chem. Int. Ed.* **2009**, *48*, 8412–8421; e) A. Walther, A. H. E. Müller, *Chem. Rev.* **2013**, *113*, 5194–5261; f) C. Tang, C. Zhang, Y. Sun, F. Liang, Q. Wang, J. Li, X. Qu, Z. Yang, *Macromolecules* **2013**, *46*, 188–193.

[3] a) T. Nisisako, T. Torii, T. Takahashi, Y. Takizawa, *Adv. Mater.* **2006**, *18*, 1152–1156; b) C. J. Behrend, J. N. Anker, B. H. McNaughton, M. Brasuel, M. A. Philbert, R. Kopelman, *J. Phys. Chem. B* **2004**, *108*, 10408–10414; c) C. J. Behrend, J. N. Anker, R. Kopelman, *Appl. Phys. Lett.* **2004**, *84*, 154–156.

[4] a) P. F. Damasceno, M. Engel, S. C. Glotzer, *Science* **2012**, *337*, 453–457; b) S. C. Glotzer, A. M. J. Solomon, *Nat. Mater.* **2007**, *6*, 557–562.

[5] a) L. Hong, A. Cacciuto, E. Luijten, S. Granick, *Nano Lett.* **2006**, *6*, 2510–2514; b) S. Jiang, Q. Chen, M. Tripathy, E. Luijten, K. S. Schweizer, S. Granick, *Adv. Mater.* **2010**, *22*, 1060–1071.

[6] M. Lattuada, T. A. Hatton, *J. Am. Chem. Soc.* **2007**, *129*, 12878–12889.

[7] a) M. C. Daniel, D. Astruc, *Chem. Rev.* **2004**, *104*, 293–346; b) J. Shan, H. Tenhu, *Chem. Commun.* **2007**, 4580–4598.

[8] a) Q. Xu, X. Kang, R. A. Bogomolni, S. Chen, *Langmuir* **2010**, *26*, 14923–14928; b) S. Pradhan, L. Xu, S. Chen, *Adv. Funct. Mater.* **2007**, *17*, 2385–2392; c) L. Xu, S. Pradhan, S. Chen, *Langmuir* **2007**, *23*, 8544–8548.

[9] a) B. Wang, B. Li, B. Zhao, C. Y. Li, *J. Am. Chem. Soc.* **2008**, *130*, 11594–11595; b) B. Li, C. Ni, C. Y. Li, *Macromolecules* **2008**, *41*, 149–155.

[10] B. Wang, B. Li, B. Dong, B. Zhao, C. Y. Li, *Macromolecules* **2010**, *43*, 9234–9238.

[11] D. M. Andala, S. H. R. Shin, H. Y. Lee, K. J. M. Bishop, *ACS Nano* **2012**, *6*, 1044–1050.

[12] T. Chen, M. Yang, X. Wang, L. H. Tan, H. Chen, *J. Am. Chem. Soc.* **2008**, *130*, 11858–11859.

[13] A. Ohnuma, E. C. Cho, P. H. C. Camargo, L. Au, B. Ohtani, Y. Xia, *J. Am. Chem. Soc.* **2009**, *131*, 1352–1353.

[14] J. Tian, J. Jin, F. Zheng, H. Zhao, *Langmuir* **2010**, *26*, 8762–8768.

[15] J. Tian, F. Zheng, H. Zhao, *J. Phys. Chem. C* **2011**, *115*, 3304–3312.

[16] J. Tian, L. Yuan, M. Zhang, F. Zheng, Q. Xiong, H. Zhao, *Langmuir* **2012**, *28*, 9365–9371.

[17] J. Tian, G. Liu, C. Guan, H. Zhao, *Polym. Chem.* **2013**, *4*, 1913–1920.

[18] L. Liu, J. Zhang, C. Wu, H. Zhao, *Macromol. Rapid Commun.* **2008**, *29*, 45–51.

[19] H. Duan, D. Wang, N. S. Sobal, M. Giersig, D. G. Kurth, H. Mohwald, *Nano Lett.* **2005**, *5*, 949–952.

[20] H. Duan, D. Wang, D. G. Kurth, H. Mohwald, *Angew. Chem.* **2004**, *116*, 5757–5760; *Angew. Chem. Int. Ed.* **2004**, *43*, 5639–5642.

[21] S. Link, M. A. EI-Sayed, *J. Phys. Chem. B* **1999**, *103*, 4212–4217.

[22] S. Link, M. A. EI-Sayed, *J. Phys. Chem. B* **1999**, *103*, 8410–8426.

[23] S. Underwood, P. Mulvaney, *Langmuir* **1994**, *10*, 3427–3430.

[24] J. N. Kizhakkedathu, R. Norris-Jones, D. E. Brooks, *Macromolecules* **2004**, *37*, 734–743.

[25] W. Feng, R. Chen, J. L. Brash, S. Zhu, *Macromol. Rapid Commun.* **2005**, *26*, 1383–1388.

[26] T. Liu, S. Jia, T. Kowalewski, K. Matyjaszewski, *Macromolecules* **2006**, *39*, 548–556.

[27] M. Zhang, L. Liu, C. Wu, G. Fu, H. Zhao, B. He, *Polymer* **2007**, *48*, 1989–1997.

[28] Y. Yang, J. Wang, J. Zhang, J. Liu, X. Yang, H. Zhao, *Langmuir* **2009**, *25*, 11808–11814.

[29] A. Walther, A. H. E. Müller, *Soft Matter* **2008**, *4*, 663–668.

[30] B. Liu, W. Wei, X. Qu, Z. Yang, *Angew. Chem.* **2008**, *120*, 4037–4039; *Angew. Chem. Int. Ed.* **2008**, *47*, 3973–3975.

[31] J. Zhang, J. Jin, H. Zhao, *Langmuir* **2009**, *25*, 6431–6437.

[32] J. Liu, G. Liu, M. Zhang, P. Sun, H. Zhao, *Macromolecules* **2013**, *46*, 5974–5984.

[33] J. van Herrikhuyzen, G. Portale, J. C. Gielen, P. C. M. Christianen, N. A. J. M. Sommerdijk, S. C. J. Meskers, A. P. H. Schenning, *Chem. Commun.* **2008**, 697–699.

Received: April 14, 2014
Revised: May 7, 2014
Published online: July 8, 2014